

# Electronic Supplemental Information

## High-throughput mechanotransduction in *Drosophila* embryos with mesofluidics

Ardon Z. Shorr,<sup>‡a</sup> Utku M. Sönmez,<sup>‡b</sup> Jonathan S. Minden,<sup>a</sup> and Philip R. LeDuc<sup>b</sup>

<sup>a</sup> Department of Biological Sciences, Carnegie Mellon University, Pittsburgh, PA.

<sup>b</sup> Department of Mechanical Engineering, Carnegie Mellon University, Pittsburgh, PA.

<sup>‡</sup> These authors contributed equally to this work.

### S1 Analytical model of sidewalls

#### Definitions

$t$  = Thickness of the wall ( $50 \times 10^{-6} \text{ m}$ )

$h$  = Height of the wall ( $251.8 \times 10^{-6} \text{ m}$ )

$L$  = Length of the wall, i.e. width ( $2 \times 10^{-2} \text{ m}$ )

$P$  = Pressure (5 PSI =  $34473.8 \text{ N/m}^2$ )

$\omega$  = Force per unit height ( $\text{N/m}$ )

$u(x)$  = Wall deflection ( $\text{m}$ )

$E$  = Young's modulus ( $\text{N/m}^2$ )

$I$  = Second moment of area ( $\text{m}^4$ )

For beams with rectangular cross-section,  $I = \frac{L \cdot t^3}{12}$

$\nu$  = Poisson's ratio:  $-\frac{d\epsilon_y}{d\epsilon_x}$ , unitless. For PDMS<sup>1</sup>,  $\nu = 0.5$

Eq. 2 Timoshenko's beam theory:

$\kappa$  = shear coefficient

$G$  = shear modulus

$A$  = cross-section area of the beam ( $t \times L$ )

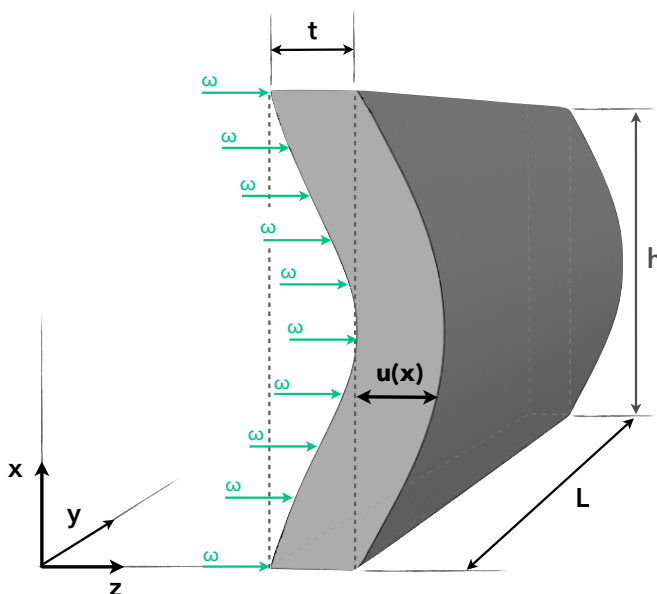


**Fig. S1 Schematic of an analytical model of deformable sidewalls.** This nomenclature is somewhat counterintuitive because we're considering a sidewall as a beam. In a beam, the region between two fixed points is the length; in a sidewall, this x-dimension is the height. Likewise, the width of a beam corresponds to the length of the channel (y), and the thickness of a beam corresponds to the width of the channel (z).

#### Shear deformation

$u_{max}$  at  $x = h/2$  can be calculated with the following conversions:

$$\omega = P \cdot L$$

$$I = \frac{L \cdot t^3}{12} \quad \text{for rectangular cross-section}$$

$$\kappa = \frac{10(1+\nu)}{12+11\nu} \quad \text{for rectangular cross-section}^2$$

$$G = \frac{E}{2(1+\nu)} \quad \text{assuming elastic and isotropic material}$$

Yielding Eq. 4 in the main text.

**Table S1** Embryo survival. Fraction of embryos observed to be larva, still developing, or dead, 24 and 48 hours after compression. Upper and lower limit of 95% confidence interval calculated by hybrid Wilson/Brown method.<sup>3</sup> N = number of embryos. P-value of two-tailed chi-square test of observed distribution compared to expected distribution from dish control.

Larva				Developing			Dead			Statistics		
At 24 hours	Mean	Upper	Lower	Mean	Upper	Lower	Mean	Upper	Lower	N	P value	Summary
Dish Control	56.8	65.6	47.5	27.0	36.0	19.6	16.2	24.2	10.5	111		
Vacuum Control	54.4	65.7	42.7	35.3	47.2	25.0	10.3	19.8	5.1	68	0.196	n.s.
7% 10 min	35.3	52.1	21.5	61.8	76.1	45.0	2.9	14.9	0.2	34	0.0001	****
22% 10 min	52.6	67.5	37.3	44.7	60.3	30.1	2.6	13.5	0.1	64	0.0001	****
7% 4 hrs	1.6	8.3	0.1	98.4	99.9	91.7	0.0	5.7	0.0	38	0.012	*
22% 4 hrs	13.0	21.0	7.8	67.0	75.4	57.3	20.0	28.9	13.3	100	0.0001	****
At 48 hours												
Dish Control	75.0	83.8	63.6	0.0	5.3	0.0	25.0	36.4	16.2			
Vacuum Control	75.0	83.8	63.6	0.0	5.3	0.0	25.0	36.4	16.2		0.438	n.s.
7% 10 min	91.2	97.0	77.0	0.0	10.2	0.0	8.8	23.0	3.0		0.028	*
22% 10 min	92.1	97.3	79.2	2.6	13.5	0.1	5.3	17.3	0.9		0.0001	****
7% 4 hrs	98.4	99.9	91.7	1.6	8.3	0.1	0.0	5.7	0.0		0.008	**
22% 4 hrs	37.0	46.8	28.2	0.0	3.7	0.0	63.0	71.8	53.2		0.0001	****

**Table S2** Simulated embryo strain at 5 PSI with varying wall thickness

Wall thickness (μm):	130	90	50	35
Young's Modulus (MPa):	1.18	1.18	1.18	1.18
Aspect Ratio:	1.94	2.80	5.04	7.19
Embryo strain:	13.1%	15.9%	22.4%	23.9%
Simulation error:	10.6%	4.2%	0.3%	3.3%

**Table S5** Inference of uniaxial compression by 10% shape change

Embryo width	Strain
195 μm	25.2%
180 μm	27.5%
160 μm	34.1%
STD	4.6
CoV	16.0%

**Table S3** Experimental embryo strain at 5 PSI with varying rigidity

Baking time (hours):	0	2.5	6	15
Young's Modulus (MPa):	1.18	1.88	2.69	3.32
Aspect ratio:	5.04	5.04	5.04	5.04
Embryo strain:	22.4%	22.0%	17.4%	15.5%
Simulation Error:	0.3%	0.2%	0.2%	0.2%

**Table S4** Consistency of uniaxial compression methods. Percent strain of embryos with max, mean, and min widths when compressed with PDMS at 5 PSI, and by simulated compression with rigid glass. The simulation was set to apply the same compressive strain to mean-width embryos as PDMS in order to test consistency.

Embryo width	PDMS	Glass
195 μm	23.7%	28.1%
180 μm	22.2%	22.2%
160 μm	19.1%	12.4%
STD	2.4%	7.9%
CoV	11.0%	38.9%

## References

- 1 R. H. Pritchard, P. Lava, D. Debruyne and E. M. Terentjev, *Soft Matter*, 2013, **9**, 6037–6045.
- 2 G. R. Cowper, *Journal of Applied Mechanics*, 1966, **33**, 335–340.
- 3 L. D. Brown, T. T. Cai and A. DasGupta, *Statistical Science*, 2001, **16**, 101–133.

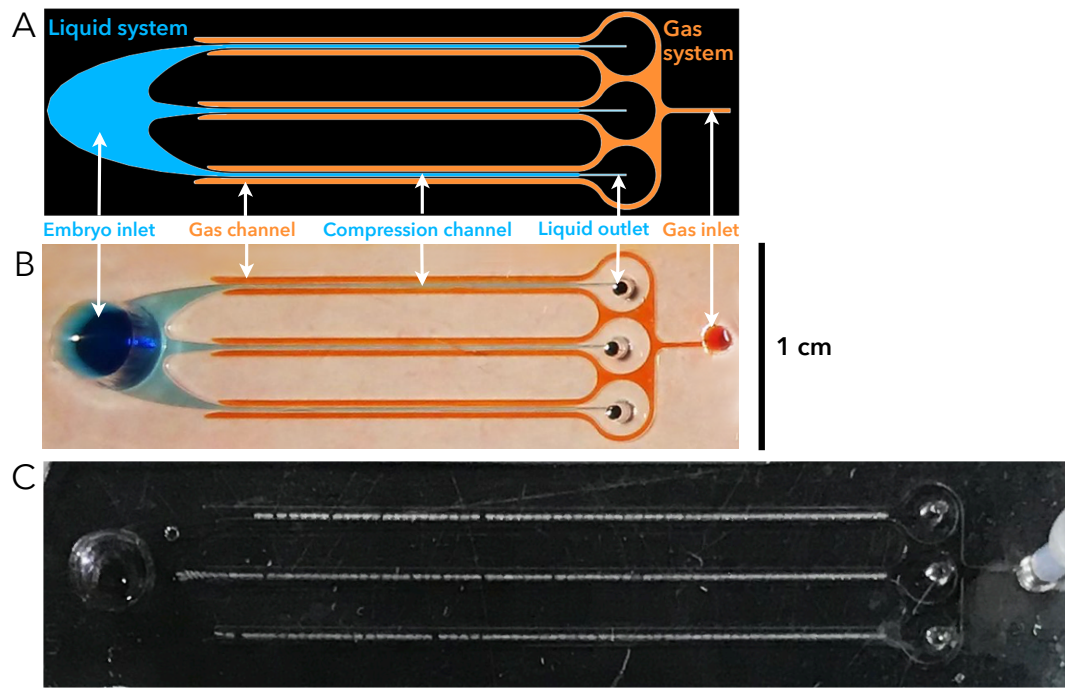


**Fig. S2 Mesofluidic PDMS compression channels.** (A) Photolithography schematic shows two interlaced microfluidic systems: an open liquid system (blue) carries embryos suspended in buffer. A closed gas system (orange) carries pressurized atmospheric air. (B) Photograph of mesofluidic channel with both systems filled with dye. (C) Photograph of *Drosophila* embryos inside a longer channel.

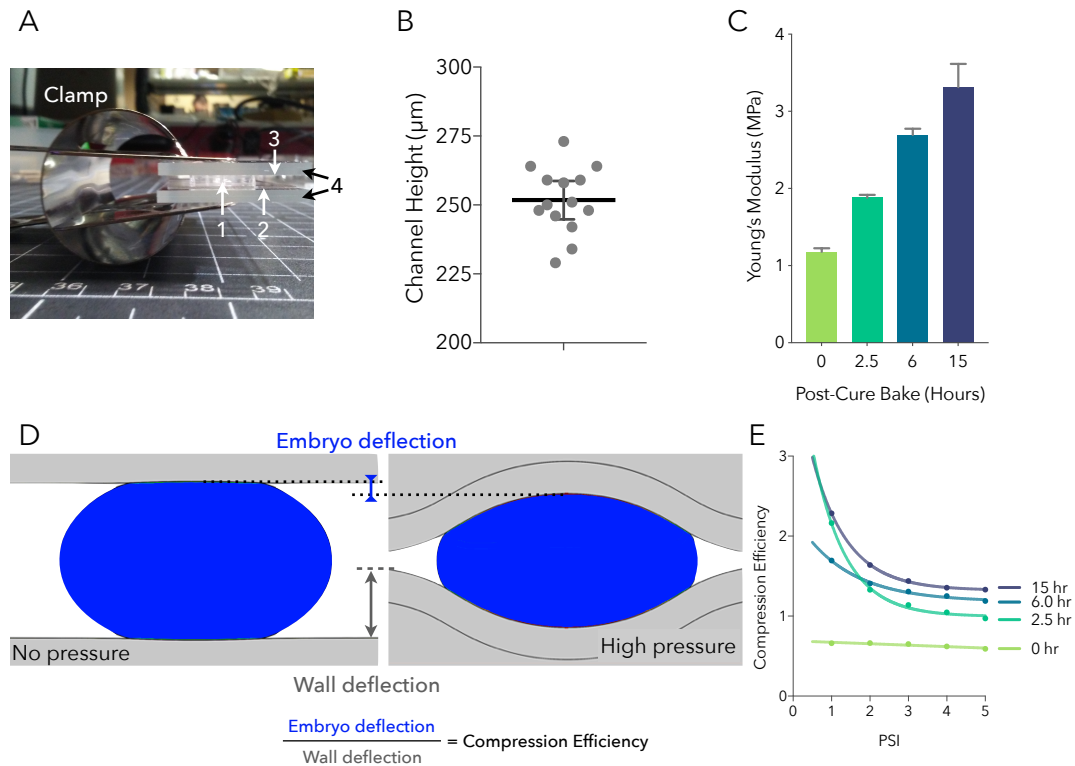


**Fig. S3** (A) Photograph of the mesofluidic device during post-bake. A polycarbonate sheet (1) covered the PDMS-glass assembly (2, 3). The assembly was held between two thick glass slides (4) and clamped to ensure physical contact between PDMS and the coverslip while curing. Marks are cm. (B) Profilometry measurements of channel height show a mean of 251.8  $\mu\text{m}$  with uniformity ( $1 - \sigma/\mu \times 100$ ) > 95%. (C) Young's modulus of 50  $\mu\text{m}$  sidewalls with differential post-cure baking. Deflection was measured at 10 points and calculated by Eq. 6. SEM bars. (D) Illustration of "compression efficiency" parameter – the ratio of embryo deflection to wall deflection. Compression efficiency measures a deformable wall's preference for compressing over wrapping. (E) Plot of compression efficiency over 5 PSI for channels with a range of post-bake durations. In the no-bake condition (0 hours), sidewalls are deflected with minimal embryo compression. As the rigidity of the walls increases, compression efficiency increases. Simulation results in Fig. S5.

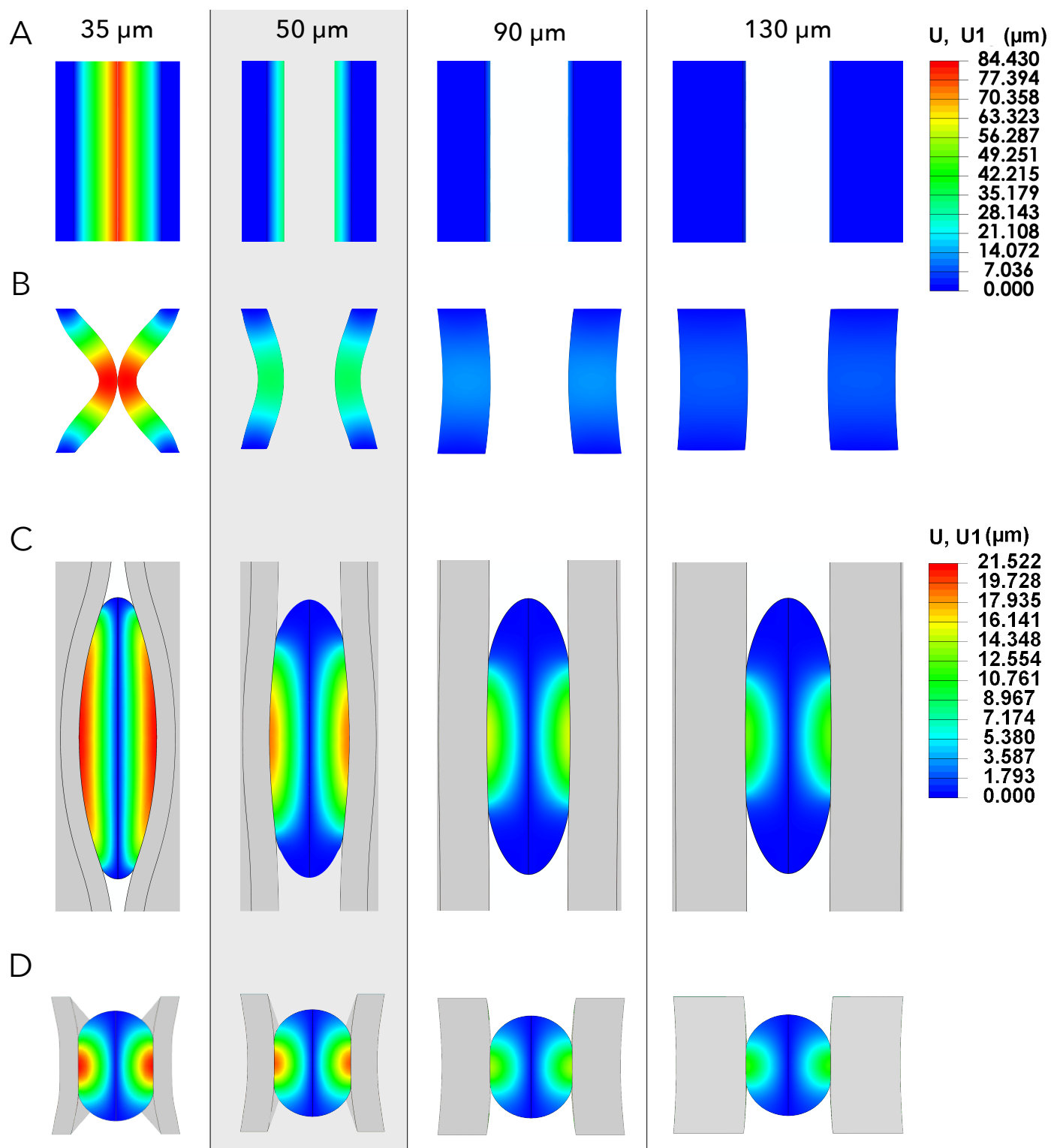


**Fig. S4** Simulation results of uniaxial node displacement at 5 PSI with variable wall thickness. (A, B) Empty channel, top view and side section. 35  $\mu\text{m}$  walls close completely. (C, D) Channel with embryo, top view and side section. 35  $\mu\text{m}$  walls showed heavy wrapping around the embryo, while 90+  $\mu\text{m}$  walls showed low displacement resulting in low compression. 50  $\mu\text{m}$  walls (shaded) were selected.



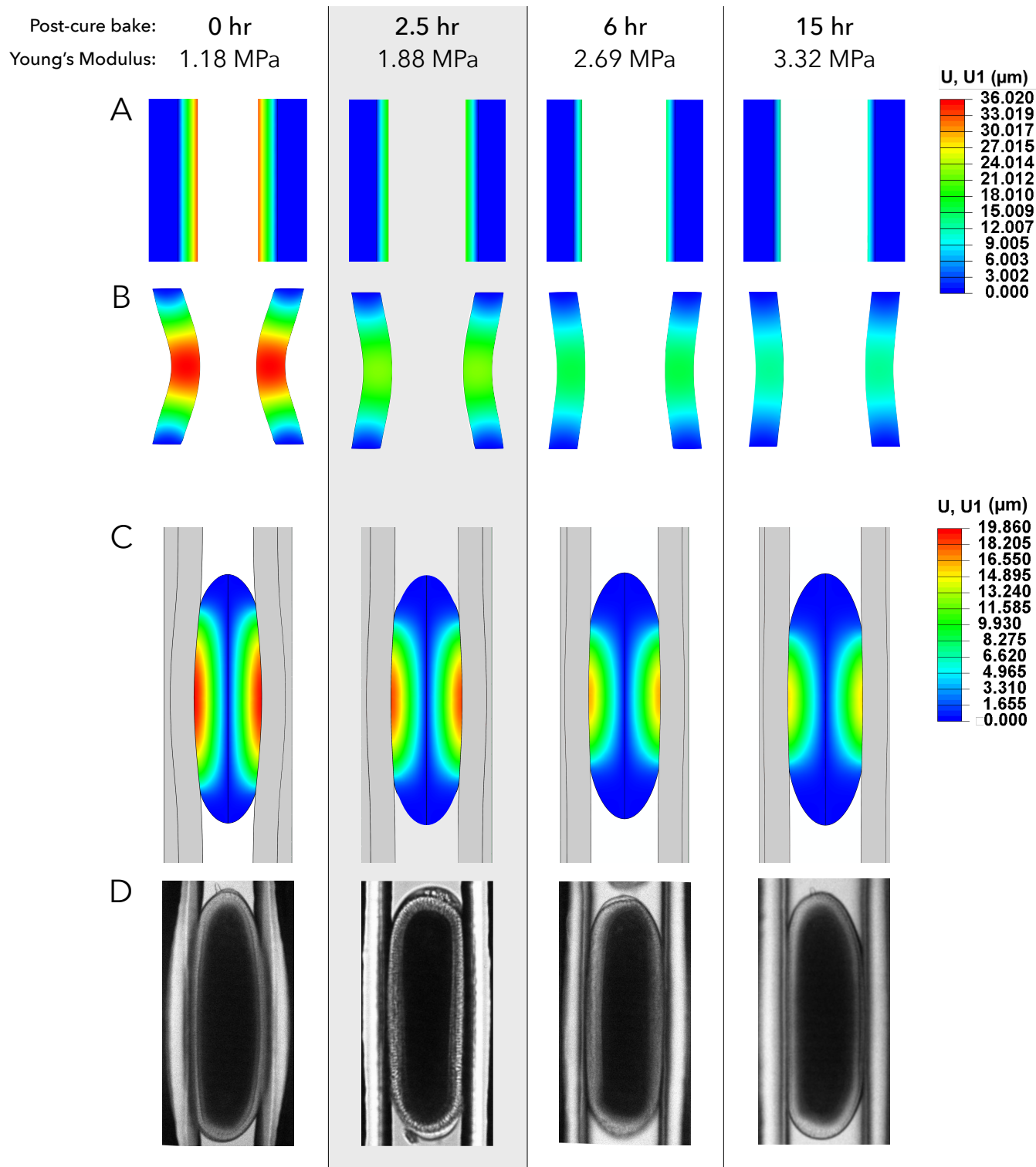


**Fig. S5 Simulation results and micrographs of embryo compression at 5 PSI with variable wall rigidity.** 50  $\mu\text{m}$  thick walls were given a range of Young's modulus as a result of variable post-bake curing times (Fig S3C). (A, B) Empty channel, top view and side section. (C) Channel with embryo, top view (side section in Fig. 2E). Less rigid walls showed greater wrapping around the embryo. (D) Micrographs from experimental results. 2.5 hour post-cure bake (shaded) was selected.

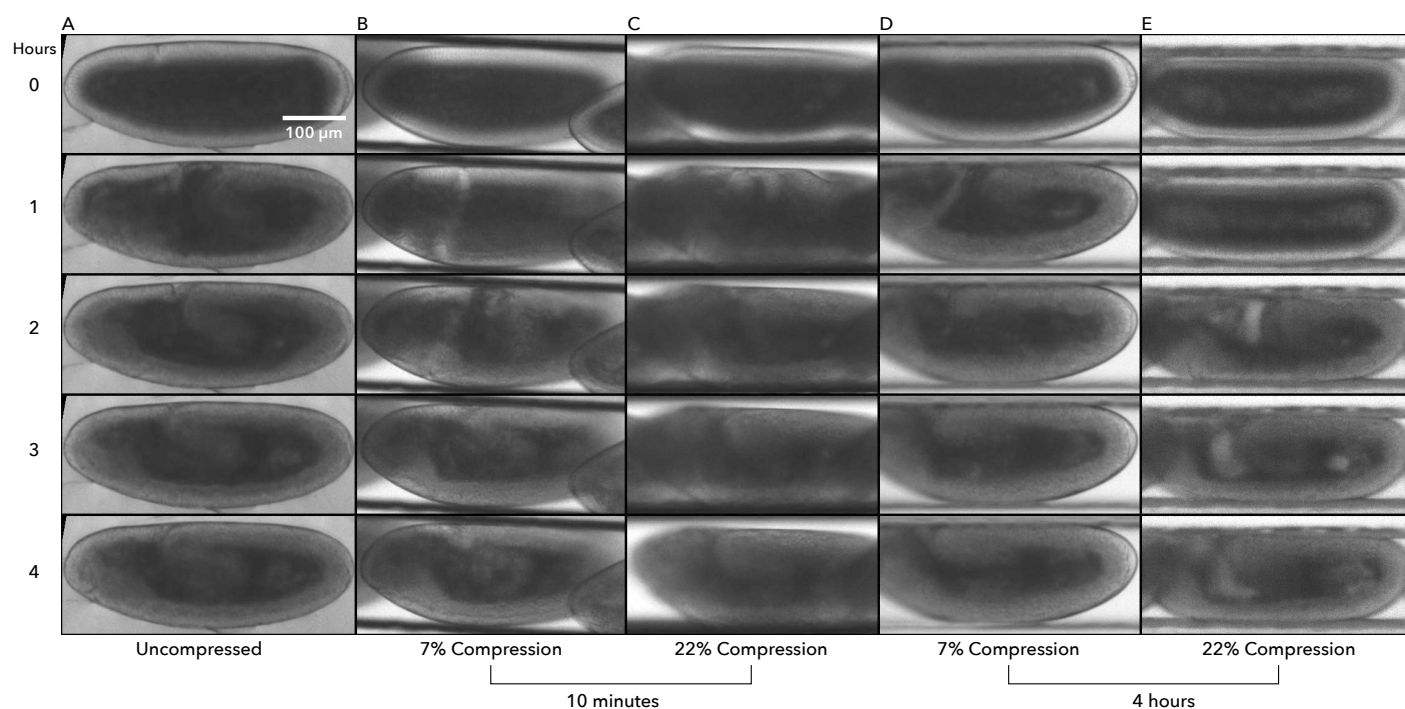


**Fig. S6** Timelapse microscopy of embryos inside the channel. DIC images taken every hour for four hours. (A) Uncompressed embryo proceeds through germ-band extension. (B–D) Compressed embryos proceed through morphological movement with some delay. (E) Some embryos compressed by 22% for 4 hours showed significant delay for 1 hour, then proceeded through germ-band extension.

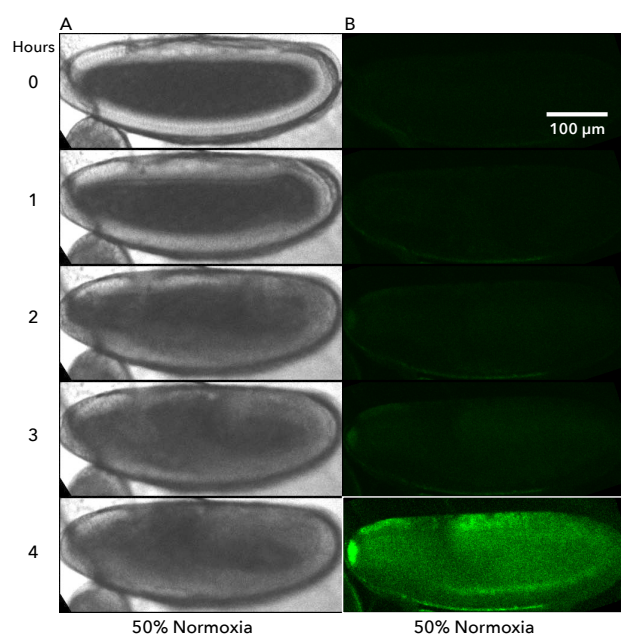


**Fig. S7** Timelapse microscopy of embryos under 50% normoxia. DIC and *twist:eGFP* fluorescence images taken every hour for four hours. The maximum and minimum pixel value settings are the same as Fig. 5 except for bottom panel (white border) to show patterning.

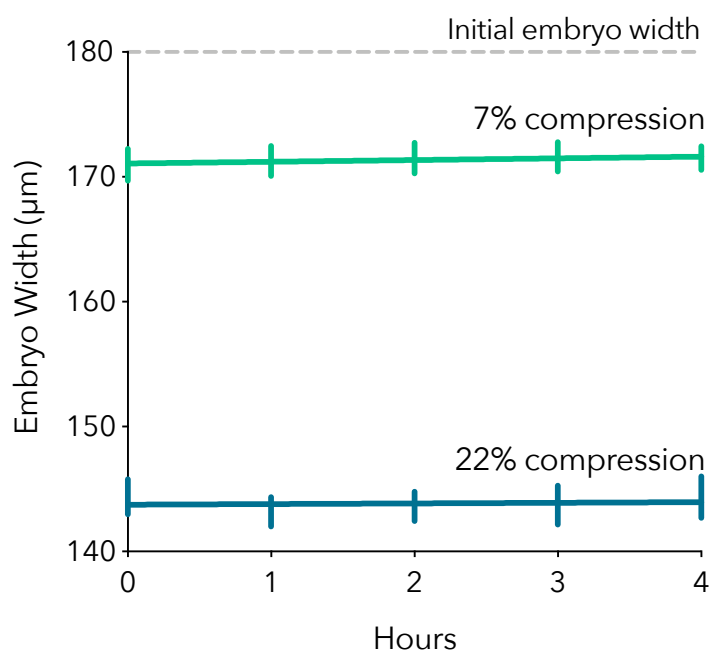


**Fig. S8** Embryo width under 7% and 22% compression over four hours, 95% confidence interval with linear fit. Embryo width is consistent, indicating steady-state elastic response over this timescale.

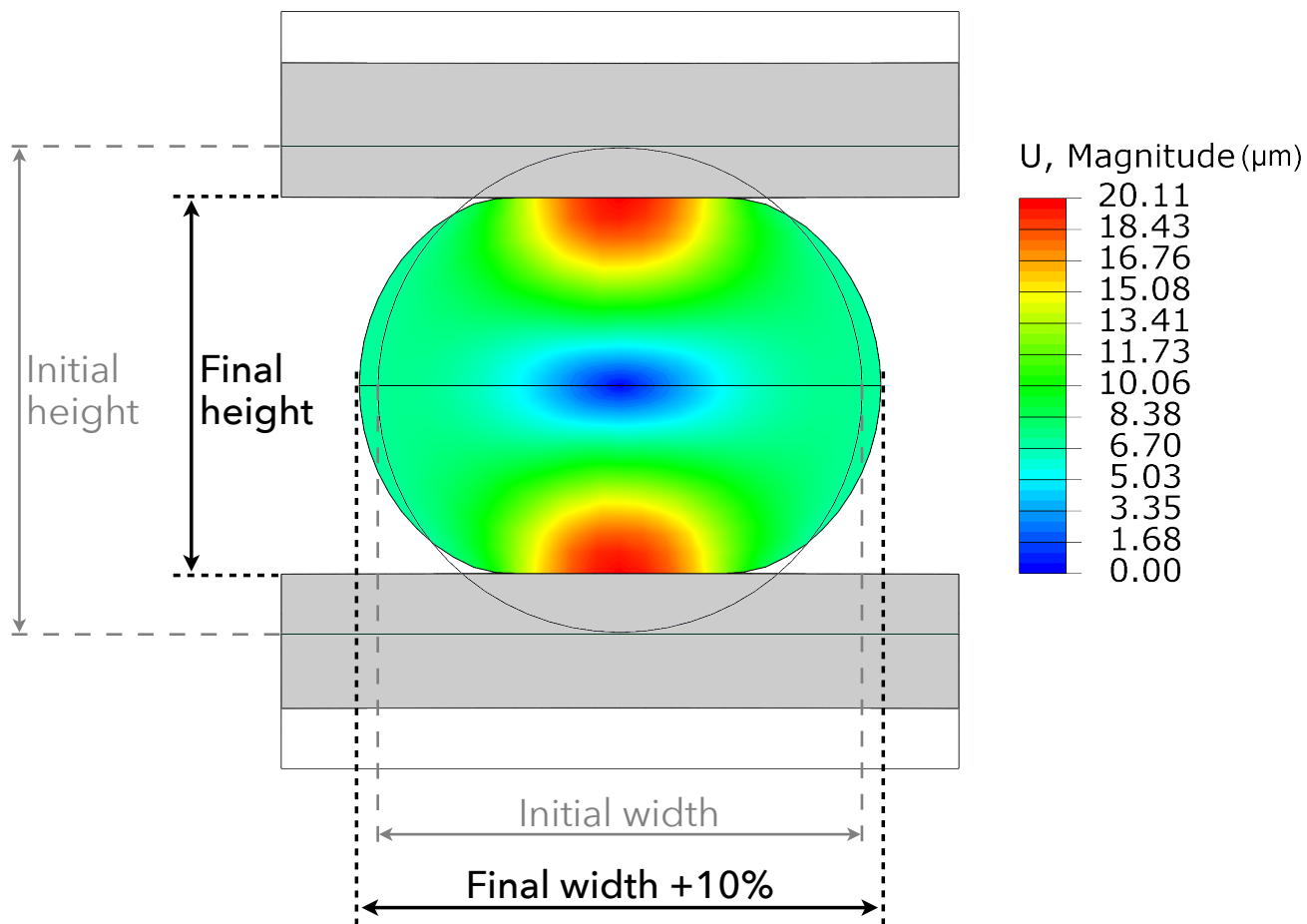


**Fig. S9** Simulation results of embryo compression between two rigid walls such that lateral expansion is 10%. Before width expands, height decreases (red). As a result, the inferred compression is substantially larger than 10% (Table ??).

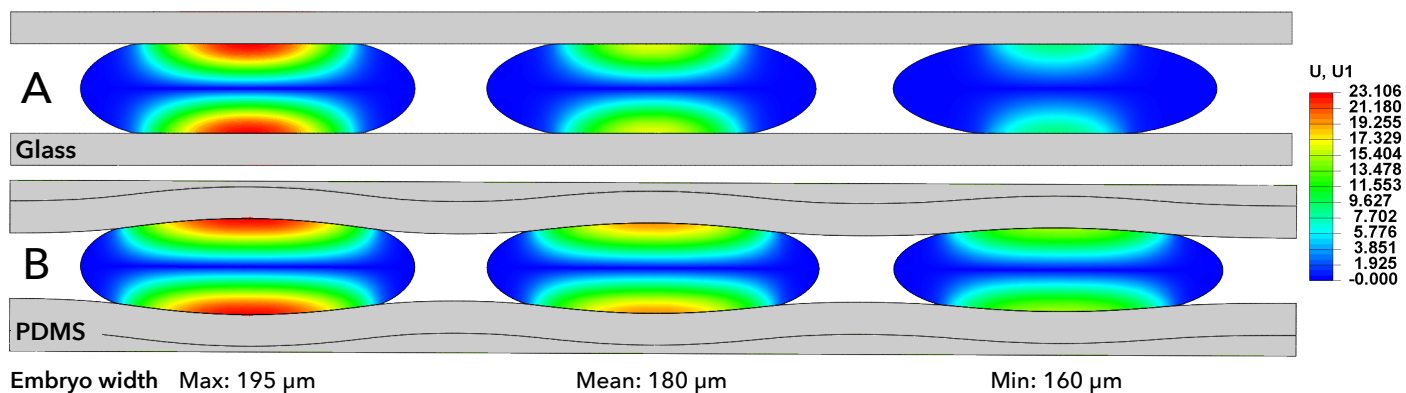


**Fig. S10** Flexible walls are more consistent than rigid glass when compressing a distribution of widths. Simulation of embryos of maximum, median, and minimum width at Stage 5. (A) When compressed by rigid glass, the channel width is consistent, applying more compression to wider embryos. (B) When compressed by flexible PDMS, the channel width is unique to each embryo, which resists deformation as a function of width. This results in a more consistent compression.